An Intercept and Following Strategy for a Multi-rotor Platform using a Modified Proportional Navigation

Conference Paper · January 2019

DOI: 10.2514/6.2019-0683

5 authors, including:

Jay Wilhelm
Ohio University
74 PUBLICATIONS **268** CITATIONS

An Intercept and Following Strategy for a Multi-rotor Platform using a Modified Proportional Navigation

Garrett S. Clem * and Jay P. Wilhelm†
Russ College of Engineering and Technology, Athens, Oh, 45701

David Casbeer‡, David Grymin§, and Isaac Weintraub¶
Control Science Center of Excellence, U.S. Air Force Research Laboratory, Wright-Patterson Air Force Base, Ohio 45433

Combatant small Unmanned Aerial Vehicles (CUAVs) can easily enter restricted airspace and may be mitigated by counter UAVs. Intercepting and following combatant UAVs in restricted airspace could be achieved with multi-rotor UAVs. A pseudotarget based Proportional Navigation (PN) guidance algorithm that guides a UAV to intercept and follow a combatant UAV using highly uncertain sensor position information was investigated. Simulations were performed to validate the model and develop a ratio of following distance to initial range. Near zero following distance was achieved for a finite range of initial line-of-sight angles.

I. Nomenclature

x	=	UAV X Position
y	=	UAV Y Position
x_T	=	Target x Position
y_T	=	Target y Position
V_T	=	Target Velocity
β	=	Target heading
x_I	=	Interceptor x Position
y_I	=	Interceptor y Position
V_I	=	Interceptor Velocity
γ	=	Interceptor heading
λ	=	Line of Sight Angle
R_{TI}	=	Range from Target to Interceptor
R_{TIx}	=	Range x Component
R_{TIy}	=	Range y Component
V_{TIx}	=	Velocity x Component
V_{TIy}	=	Velocity y Component
$\dot{\gamma}$	=	Interceptor heading Rate
$\dot{\lambda}$	=	Line of Sight Rate
N	=	Guidance Gain
b	=	Minimum Uncertainty Radius

II. Introduction

Tracking and following small Unmanned Aerial Systems (sUAS) have applications in autonomous flight formation, swarming, and standoff target tracking. Multi-rotor sUAS may also be guided to passively track and follow another

*Graduate Research Assistant,Mechanical Engineering, 251 Stocker Center Athens, Oh, and AIAA Member Grade (if any) for first author.
†Assistant Professor, Mechanical Engineering, 251 Stocker Center Athens Oh, 45701, Senior Member
‡Team Lead UAV Cooperative & Intelligent Control, Associate Fellow
§Research Engineer, Senior Member
¶Research Engineer, Senior Member

target sUAS flying in restricted airspace. Path planning [1, 2], heading control laws [3], and Line-Of-Sight (LOS) guidance algorithms [4] have been proposed for intercepting and following moving targets. Path planning is typically performed at a ground station requiring constant communication to adapt for a moving target. Control laws for target tracking rely on low uncertainty target position estimates [5]. LOS methods such as PN guidance has been used in missile systems to track targets [6], but may fail to follow a target under head-on intercept scenarios. Direction and range to the target can be measured with on-board sensors but provide highly uncertain estimates due to limitations in the sensing technology. The focus of this paper was to investigate vehicle intercept and tracking performance when the target position is highly uncertain.

A pseudotarget PN guidance algorithm that directs a sUAS to intercept and follow a target sUAS using uncertain position information was investigated. First the interceptor and target kinematics are presented along with the unmodified PN guidance algorithm. Next an on-board sensor that measures the target's position, which has some uncertainty, is modeled. A state machine pseudotarget is than introduced that intercepts and follows a target with high initial position uncertainty for head-on and tail-chase scenarios. Simulations were performed to validate the model and to show that the following distance can be predicted from the initial LOS angle, range, and sensor characteristic.

A. Literature

Tracking an aerial target has been achieved by implementing closed-loop feedback systems [3], path following guidance [1, 2], and LOS guidance algorithms [7]. Closed-loop position and velocity control of a multi-rotor for following a ground target with intermittent and noisy vision data was achieved in [4]. Vision systems are promising, buy may suffer from field of view distance limitations and are sensitive to differential lighting conditions. Following time varying paths and intercepting multiple ground targets was demonstrated in [8] by introducing a heading control law. Distance to the target at interception varied an order of magnitude and required the target position.

Target tracking without modification of a UAV's control system has been accomplished by framing target tracking as a path planning problem. A waypoint generation technique was developed in [1] that satisfied fixed wing forward velocity constraints while maintaining the target in the field-of-view. Sub-optimal placement of waypoints resulted in exaggerated trajectories for fixed wings when tracking an accelerating target. Multi-rotors tracked the target with less error when navigating waypoints for the same scenario due to the multi-rotors ability to hover. Less exaggerated trajectories for tracking a maneuvering target was accomplished for a fixed wing UAV in [9]. An optimal path planning strategy consisting of a Markov Decision Process and cost based state reduction showed less tracking error in comparison to lookup tables and heuristic methods, but took considerably longer to provide a solution [10]. Target tracking with path planning techniques may require the UAV to be in constant contact with the ground station where planning typically occurs.

Target tracking may also be accomplished by implementing LOS guidance methods, such as those used in missiles [7]. LOS methods control the missile's velocity to be on a collision triangle with the target [11, 12]. Adapting a pure pursuit LOS guidance to chase a target with less tracking error than traditional pure pursuit guidance was demonstrated in [13]. PN guides a missile to a target by nulling the LOS rate [11, 12]. PN guidance has had continued interest and may have new uses such as cooperative defense strategies [6]. The PN guidance law controls a missile to intercept a target but does not contain arguments to command a specific approach angle. Ratnoo and Ghose modified the PN guidance gain throughout flight to satisfy a terminal angle constraint [14]. Oza and Padhi discuss how time varying guidance gains result in singularities near the end of the flight and provide an impact-angle-constrained suboptimal model predictive static programming guidance [15]. Optimal impact-angle-constrained guidance algorithms have been developed for 2D [16] and 3D [17] engagements. The impact-angle constrained guidance in literature typically does not consider the tracking performance for following a target after intercept. Guidance singularities at interception caused by a rapid LOS rate increase are also often ignored since the objective is to impact the target. The final following distance for a sUAS pursuing a non-evading target is presented along with a pseudotarget based PN guidance that avoids LOS rate singularities.

III. Model

A. Intercept Model

An interceptor and target were modeled as Dubins vehicles [18] in $\mathbb{R}^2$ with x representing East and y altitude, shown in Figure 1. UAV position $[x \quad y]^T$ was determined from the integral of the velocity $[\dot{x} \quad \dot{y}]^T$ shown in Equation 1. The heading of both sUAS was the input u and was bounded on the interval $[0, 2\pi)$. The non-maneuvering target heading β was a constant while interceptor heading γ was determined by PN guidance. The line-of-sight angle λ is the angle between the interceptor and target with respect to the positive x axis.

$$\begin{aligned} \dot{x} &= v\cos(\phi) \\ \dot{y} &= v\sin(\phi) \end{aligned} \tag{1}$$

$$\phi = u \tag{2}$$

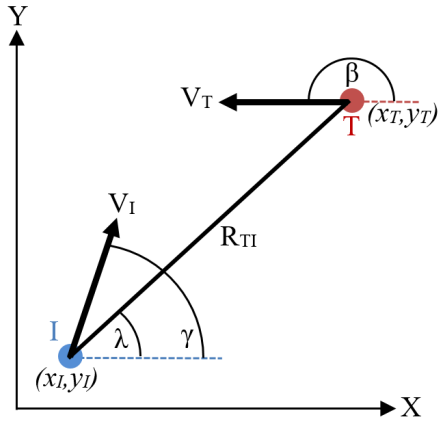

Fig. 1 Interceptor and Target Engagement Scenario (x-East, y-Up)

The PN guidance law operates on the principle of proportionally controlling heading so that the LOS $\dot{\lambda}$ is driven to zero. The input rate $\dot{u}$ is proportional to the LOS rate and a fixed guidance gain N. Second order Runge-Kutta integration is typically used to determine u from Equation 3.

$$\dot{u} = N\dot{\lambda} \tag{3}$$

Guidance gains of $N < 3$ are generally referred to as conservative, while $N > 5$ are referred to as more aggressive [7]. Conservative gains result in larger turn radii whereas larger gains result in smaller turn radii. Multi-rotors are capable of making abrupt heading changes in comparison to fixed wing UAVs and it was assumed a guidance gain of $N = 5$ is not beyond multi-rotor capability. The resulting guidance is expected to return sharp turns and straight line optimal paths when used with the Dubins kinematic model. The LOS angle and rate are calculated in Equations 4 and 5 respectively.

$$\lambda = \tan^{-1}\left(\frac{y_T - y_I}{x_T - x_I}\right) \tag{4}$$

$$\dot{\lambda} = \frac{(x_T - x_I)(V_{Ty} - V_{Iy}) - (y_T - y_I)(V_{Tx} - V_{Ix})}{(x_T - x_I)^2 + (y_T - y_I)^2} \tag{5}$$

Range is the Euclidean distance between the target and the interceptor, shown in Equation 6.

$$R_{TI} = \sqrt{(x_T - x_I)^2 + ((y_T - y_I)^2} \tag{6}$$

PN guidance is effective at reducing the range between the interceptor and the target, however it does not always setup the interceptor to follow once the range is at a minimum. For head-on intercept shown in Figure 2a and 2b the LOS rate experiences a singularity and fails to follow the target. The singularity is caused by a combination of relative velocity sign change and division by zero. Solutions around the singularity can be obtained for a linearized proportional navigation [19] but are not a concern for traditional missile systems because the mission is complete when the range is near zero. For an intercepting UAV with the intention of following the target, a singularity calls for control efforts beyond the saturation point. After the singularity occurs there remains a possibility for the nulled LOS condition to be met even if the interceptor and target are heading away from each other. Figure 2a demonstrates how for head-on intercepts the nulled LOS rate can be satisfied and the interceptor flys away from the target. Figure 2b shows how a singularity can occur near zero range.

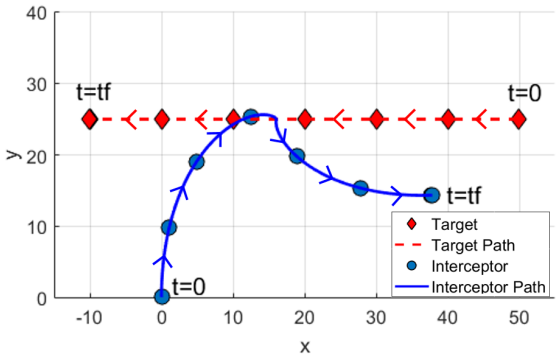

(a) Failed follow for head on intercept

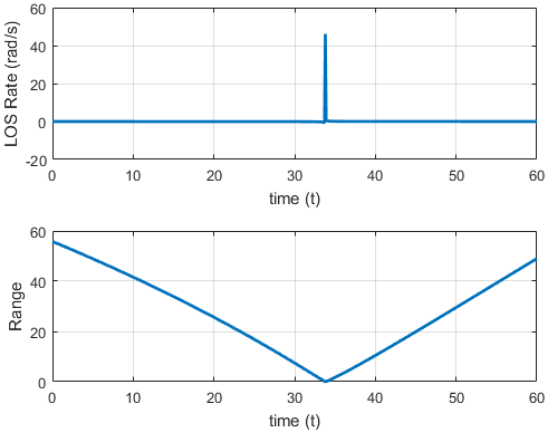

(b) Failed follow with LOS-rate singularity and range

Fig. 2 Intercept and Following Example of Failure

The interceptor successfully intercepts and follow the target for a tail-chase scenario shown in Figure 3a and no singularities are present in Figure 3b. The tail-chase scenario has the added benefit of placing the interceptor behind the target, allowing for a transition into a follow. The elimination of the singularity and easy transition into a follow make a case for waiting on the target before intercepting it directly, which is the motivation for introducing a pseudotarget into the PN guidance model.

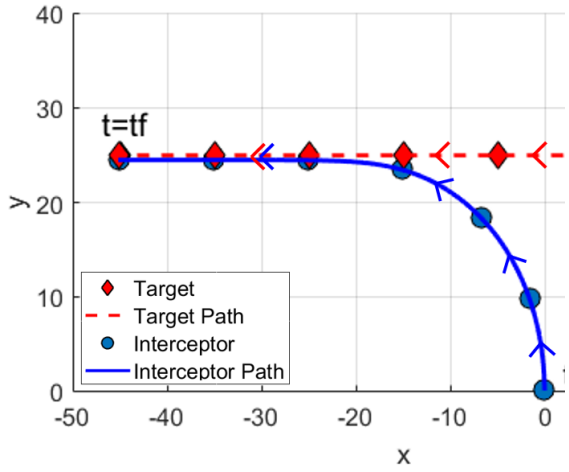

(a) Successful follow for tail chase intercept

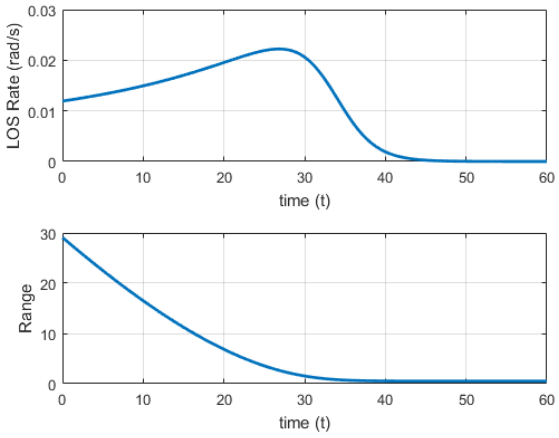

(b) Successful follow LOS-rate and range

Fig. 3 Intercept and Following Example of Success

B. Intercept and Follow Model

The LOS rate and range uncertainties in x and y are assumed to be equal, therefore the actual position of the target is in the space $(x_T \pm r, y_T \pm r)$, where r is the radius of uncertainty. Figure 4 shows a representation of the measurement as a point centered in a circle of radius r. The region inside the circle is the space where the target may actually exist. The interceptor should avoid the inside of the circular region to prevent an unintended collision with the target. The uncertainty decreases linearly as a function of range as shown in Equations 7 and 8.

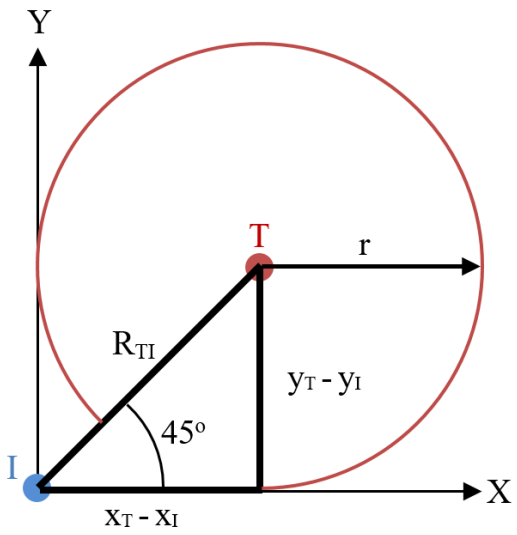

Fig. 4 Position uncertainty radius centered on target

$$r = dr\sqrt{(x_T - x_I)^2 + (y_T - y_I)^2} + b \tag{7}$$

$$b = r_0 - dr\sqrt{(x_{T0} - x_{I0})^2 + (y_{T0} - y_{I0})^2} \tag{8}$$

Sensing of range and direction was modeled as a function of the range R_{TI}, rate of change dr, and the minimum uncertainty radius b. A pseudotarget was introduced into the engagement scenario which prevents the interceptor from entering the region of uncertainty while maintaining the requirements of intercepting and following the target. The modified guidance was developed to satisfy a small range of scenarios where the target travels at constant heading, altitude, and speed equal to that of the interceptor. The interceptor avoids the region of uncertainty while following and intercepting the target by pursuing a pseudotarget.

The pseudotarget acted as a state machine consisting of $wait$, $intercept$, and $follow$ states shown in Figures 5a, 5b, and 5c respectively. When the minimum altitude of the uncertainty is below the horizon $y_I - r < 0$ the pseudotarget's state is set to $wait$ and waits at it's current position. Uncertainty decreases as the target approaches the interceptor eventually satisfying the condition $y_I - r > 0$ triggering a change in state from $wait$ to $intercept$. When the $intercept$ state is active the pseudotarget is placed at the minimum uncertainty $y = y_T - r$ with no movement in the x axis, $x = 0$. Placing the pseudotarget at the minimum uncertainty altitude prevents the possibility of an unintended collision with the target. Intercept is intended to reduce the range to the target and get close, but not result in a collision. Once $x_T < x_I$ the problem becomes a tail chase scenario and the risk of collision is non existent. The algorithm is set to the $follow$ state where the pseudotarget is placed on top of the targets estimated position.

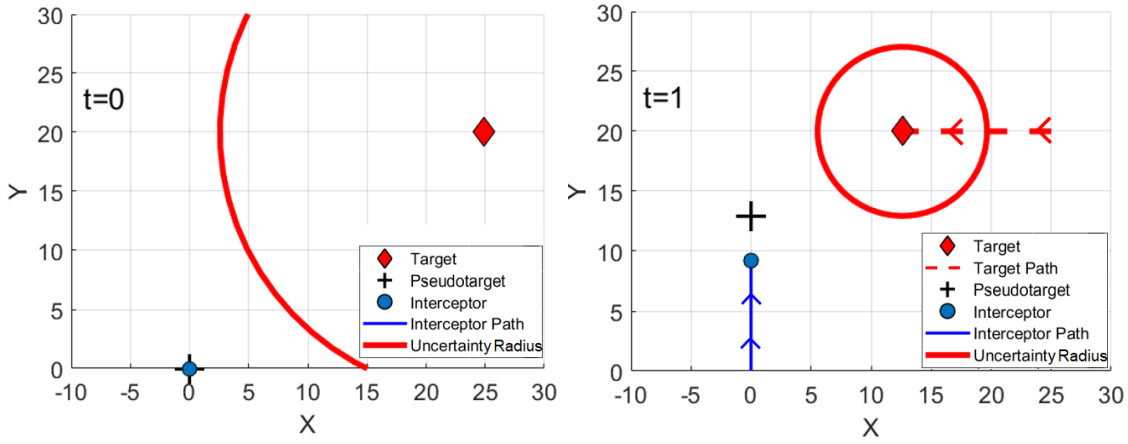

(a) Wait

(b) Intercept

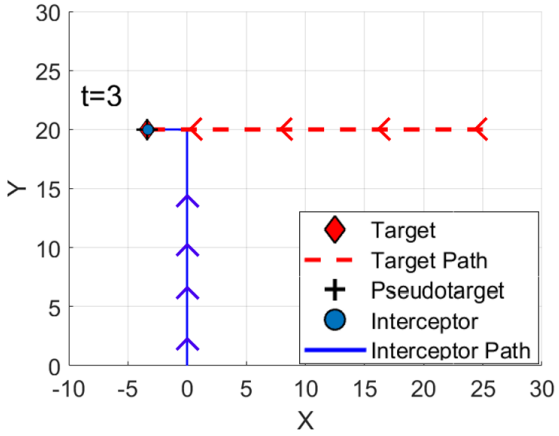

(c) follow

Fig. 5 Interception Phases

With the target moving at constant altitude and both vehicles sharing the same velocity, it is expected that the following distance will be near zero if the intercept is active when $x_T \geq y_T$. If the intercept occurs when $x_T < y_T$, the interceptor is at a disadvantage and will fail to close the distance. The sensor was modeled so that the uncertainty circle is above the horizon once the target has crossed the $x = y$ line by calculating an appropriate initial uncertainty r_0. Referring back to Figure 4 a target at a LOS of 45°, has an altitude of R_{TI_y}, and an initial uncertainty radius r_0. Determining the initial radius was done geometrically in Equations 9 and 10 and was set to 0.7 times the initial range.

$$\sin(45^\circ) = \frac{y_T - y_I}{\sqrt{(x_T - x_I)^2 + (y_T - y_I)^2}} \tag{9}$$

$$(y_T - y_I) = \sqrt{(x_T - x_I)^2 + (y_T - y_I)^2}\,\sin(45^\circ) \tag{10}$$

$$r_0 = 0.7 R_{TI} \tag{11}$$

The impact of r_0 on following distance can be seen in Figures 6a and 6. Each Figure shows the results of three target initial conditions along the $x = y$ line. Figure 6a shows a near zero following distance for a r_0 ratio of $0.7R_{TI}$. When $r_0 > 0.7R_{TI}$ the following distance becomes less predictable and is not constant along the target initial conditions on the $x = y$ line as shown in Figure 6.

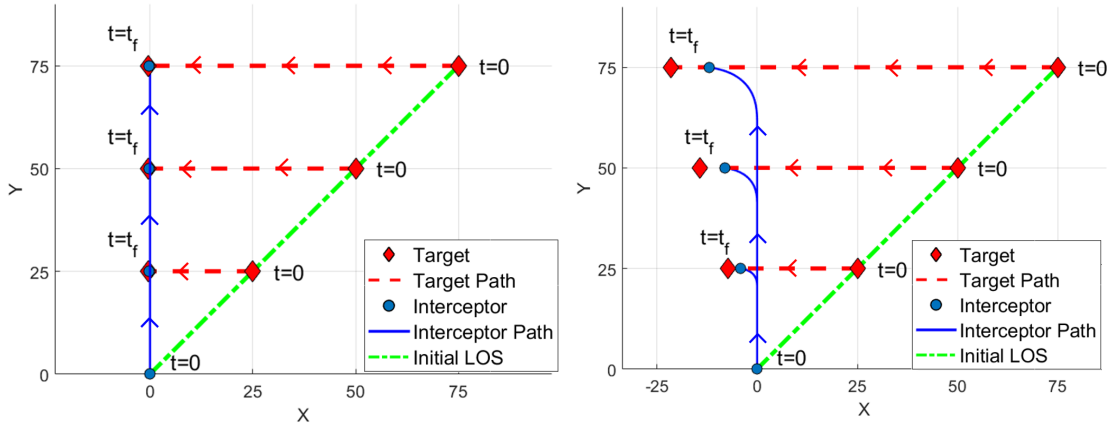

(a) Initial uncertainty ratio $0.7R_{TI}$ results in consistent following distance

(b) Initial uncertainty ratio $> 0.7R_{TI}$ results in increasing following distance as initial range increases

Fig. 6 Results of Following Distance

The modified pseudotarget PN guidance was given the same initial conditions as shown in Figure 2a and the performance compared. Traditional PN guidance performed well during the tail-chase but failed to follow the target and experienced a LOS singularity for a head-on intercept. The PN guidance with a psuedotarget successfully intercepts and follows the target, Figure 7a, with non-singularity LOS rates, shown in Figure 7b. Traditional PN out performed the pseudotarget PN guidance for target initial condition $x_T = 15$ which demonstrates that a single guidance algorithm may not be suitable for all cases and a decision on which algorithm to use for a given set of initial conditions should be made. Table 1 summarizes the performance of the algorithms for the two initial conditions.

Table 1 Traditional PN and Pseudotarget PN Following Distance and LOS rate

	Following Distance	Max LOS Rate (rad/s)
Traditional PN	0.51	0.02
	FAILED	46.07
PN with Pseudotarget	6.51	0.06
	0.88	0.04

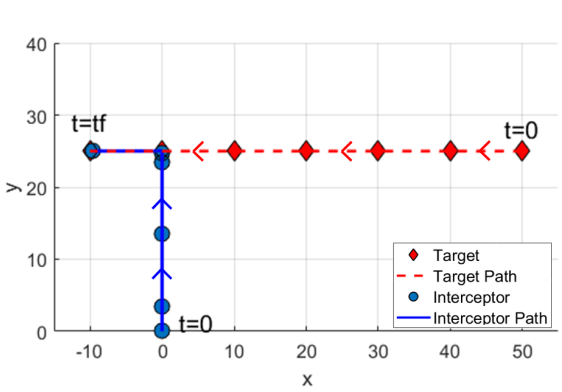

(a) Target and Interceptor Position

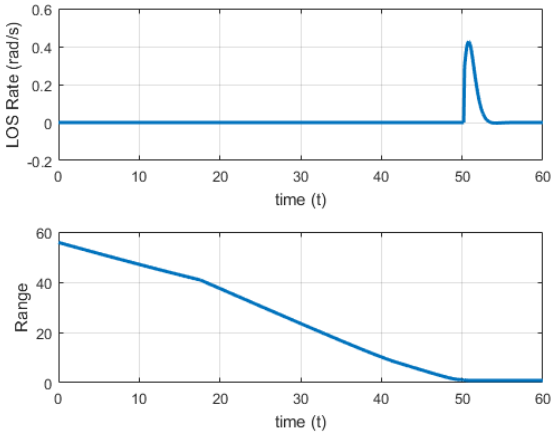

(b) LOS and Range Performance

Fig. 7 Tail chase with no singularities, and steady state range $R_{TI} \approx 0$

IV. Simulations

The pseudotarget state machine PN guidance was validated through MATLAB simulations and a ratio for predicting following distance as a function of initial LOS, range, and sensor characteristic is presented for a non maneuvering target. Initial target conditions of $x = [-100, 100]$ $y = [10, 100]$ in one unit increments were evaluated with a constant heading of $\beta = 180°$. Initial uncertainty radius of the target estimate for each scenario was 0.7 times the initial range with rate of change $dr = 1$. Interceptor initial conditions remained constant where the initial position and heading were $(0, 0)$ and 90° respectively. Each UAV was given the same velocity so that the speed ratio of the two vehicles was 1:1. When the interceptor's heading $\gamma = \beta$ the simulation was terminated and the final positions of the vehicles recorded. Dividing the following distance by the initial range to the target produces a Following Distance Initial Range (FRIR) ratio ζ, shown in Equation 12 which can be used to describe the performance of the model.

$$\zeta = \sqrt{\frac{(x_{Tf} - x_{If})^2 + (y_{Tf} - y_{If})^2}{(x_{T0} - x_{I0})^2 + (y_{T0} - y_{I0})^2}} \tag{12}$$

The unit-less ratio ζ in the simulation space is shown in the contour plot Figure 8. Each target initial condition corresponds to a FDIR ratio on the plot, ranging from 0 to 1.65. ζ is constant along each initial LOS which allows for the prediction of following distance based on initial LOS, range, and sensor dr. Initial LOS angles less than 45° yield a ζ of near zero indicating that the following distance was near zero. Increasing LOS angles greater than 45° result in progressively higher ratios indicating an increasing following distance.

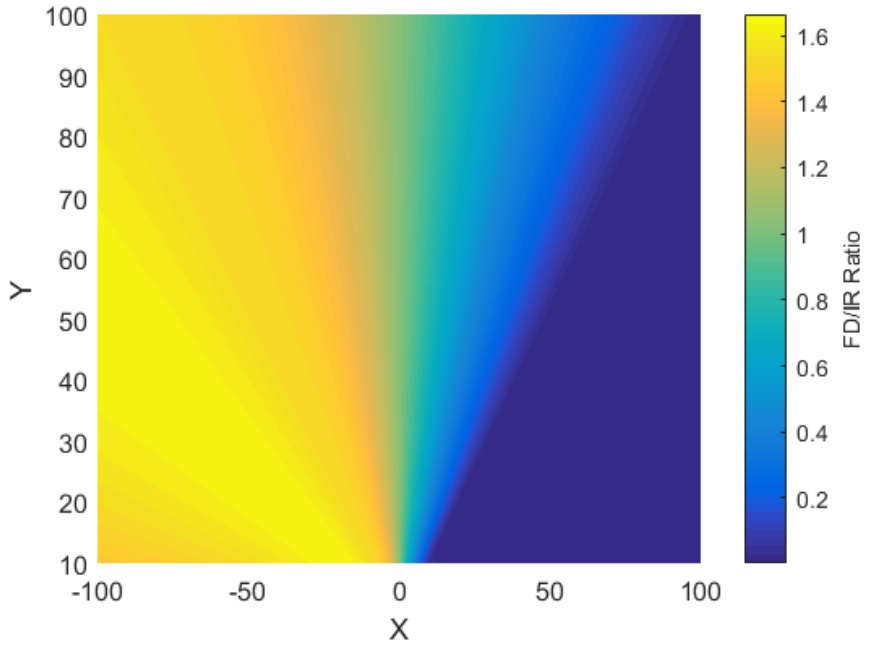

Fig. 8 Following distance to initial range ratio constant along each initial LOS

Representation of the models performance for a range of sensor dr's is shown in Figure 9. Simulations were performed for initial LOS angles ranging from 0° to 180° and sensors with dr ranging from 0.5 to 1 in 0.5° and 0.01 unit increments respectively. Sensors with $dr < 0.5$ would not allow the interceptor to reduce the following distance much farther than the initial range for nearly all LOS angles. Sensors with $dr \geq 1$ the following distance can be reduced to nearly zero for initial LOS angles between 0 and 45°.

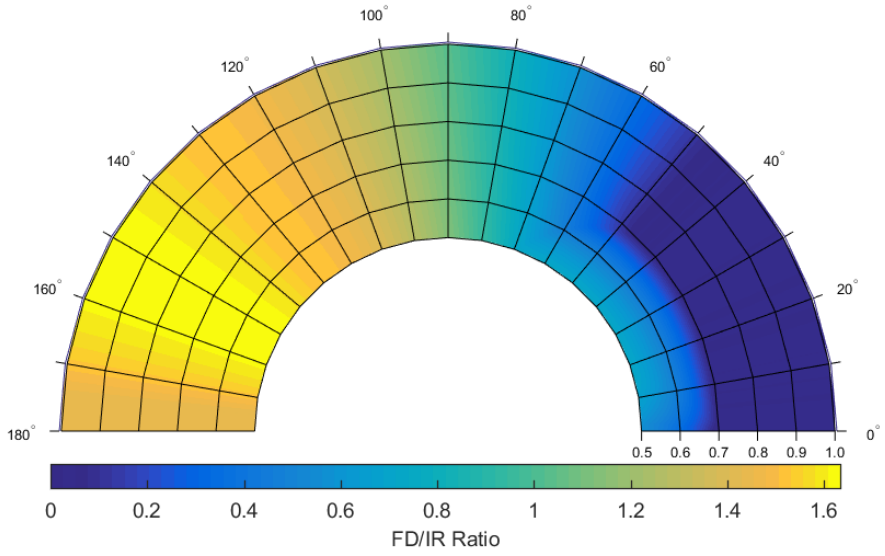

Fig. 9 Following distance to initial range ratio for multiple sensor dr confirm predicted near zero following distance for initial LOS $\leq 45°$

V. Conclusion

A pseudotarget based proportional navigation (PN) guidance algorithm that directs a UAV to intercept and follow a target UAV using highly uncertain sensor position information was investigated. Simulations were performed to determine the following distance for a finite space. Near zero following distance was achievable for a finite range of initial headings and sensor dr's. Following distance to initial range ratios indicate that the modified guidance performs optimally when the initial LOS angle is less than 45° and larger initial sight angles may benefit from other intercept methods. The state machine pseudotarget PN guidance algorithm was specifically designed to intercept and follow an inbound non-maneuvering target for the edge case of $1:1$ speed ratio. Initial results suggest that the proposed guidance is tracks the target with less error compared to traditional PN for head-on intercepts but slightly underperformed in the tail-chase scenario.

VI. Acknowledgments

The research presented was funded by Wright-Patterson Air Force Research Laboratory under the Summer Faculty Fellowship Program.

References

[1] Ariyur, K. B., and Fregene, K. O., "Autonomous tracking of a ground vehicle by a UAV," *American Control Conference, 2008*, IEEE, 2008, pp. 669–671.

[2] Beard, R. W., McLain, T. W., Goodrich, M. A., and Anderson, E. P., "Coordinated target assignment and intercept for unmanned air vehicles," Vol. 18, No. 6, 2002, pp. 911–922.

[3] Ryoo, C.-K., Cho, H., and Tahk, M.-J., "Optimal Guidance Laws with Terminal Impact Angle Constraint," Vol. 28, No. 4, 2005, pp. 724–732. doi:10.2514/1.8392, URL http://arc.aiaa.org/doi/10.2514/1.8392.

[4] Teuliere, C., Eck, L., and Marchand, E., "Chasing a moving target from a flying UAV," *Intelligent Robots and Systems (IROS), 2011 IEEE/RSJ International Conference on*, IEEE, 2011, pp. 4929–4934.

[5] Frew, E. W., "Cooperative standoff tracking of uncertain moving targets using active robot networks," *Robotics and Automation, 2007 IEEE International Conference on*, IEEE, 2007, pp. 3277–3282. URL http://ieeexplore.ieee.org/abstract/document/4209596/.

[6] Weintraub, I., Garcia, E., Casbeer, D., and Pachter, M., "An Optimal Aircraft Defense Strategy for the Active Target Defense Scenario," *AIAA Guidance, Navigation, and Control Conference*, 2017, p. 1917.

[7] Zarchan, P., and Seebass, A., *Fundamentals of Tactical Missile Guidance*, Vol. 157, AIAA Reston, VA, 1994.

[8] Oliveira, T., Aguiar, A. P., and Encarnacao, P., "Moving Path Following for Unmanned Aerial Vehicles With Applications to Single and Multiple Target Tracking Problems," *IEEE Transactions on Robotics*, Vol. 32, No. 5, 2016, pp. 1062–1078. doi:10.1109/TRO.2016.2593044, URL http://ieeexplore.ieee.org/document/7553466/.

[9] Lee, J., Huang, R., Vaughn, A., Xiao, X., Hedrick, J. K., Zennaro, M., and Sengupta, R., "Strategies of path-planning for a UAV to track a ground vehicle," *AINS Conference*, Vol. 2003, 2003.

[10] Baek, S. S., Hyukseong Kwon, Yoder, J. A., and Pack, D., "Optimal path planning of a target-following fixed-wing UAV using sequential decision processes," IEEE, 2013, pp. 2955–2962. doi:10.1109/IROS.2013.6696775, URL http://ieeexplore.ieee.org/document/6696775/.

[11] Shneydor, N. A., *Missile guidance and pursuit: kinematics, dynamics and control*, Elsevier, 1998.

[12] Yanushevsky, R., *Modern missile guidance*, CRC Press, 2007.

[13] Yamasaki, T., Enomoto, K., Takano, H., Baba, Y., and Balakrishnan, S. N., "Advanced pure pursuit guidance via sliding mode approach for chase UAV," *Proceedings of AIAA Guidance, Navigation and Control Conference, AIAA*, Vol. 6298, 2009, p. 2009.

[14] Ratnoo, A., and Ghose, D., "Satisfying terminal angular constraint using proportional navigation," *Proceeding of AIAA Guidance, Navigation, and Control Conference*, 2009, pp. 1–24.

[15] Oza, H. B., and Padhi, R., "Impact-angle-constrained suboptimal model predictive static programming guidance of air-to-ground missiles," *Journal of Guidance, Control and Dynamics*, Vol. 35, No. 1, 2012, pp. 153–164.

[16] Park, B.-G., Kim, T.-H., and Tahk, M.-J., "Optimal impact angle control guidance law considering the seeker's field-of-view limits," *Proceedings of the Institution of Mechanical Engineers, Part G: Journal of Aerospace Engineering*, Vol. 227, No. 8, 2013, pp. 1347–1364.

[17] Kumar, S. R., and Ghose, D., "Three dimensional impact angle constrained guidance law using sliding mode control," *American Control Conference (ACC), 2014*, IEEE, 2014, pp. 2474–2479.

[18] Dubins, L. E., "On Curves of Minimal Length with a Constraint on Average Curvature, and with Prescribed Initial and Terminal Positions and Tangents," Vol. 79, No. 3, 1957, p. 497. doi:10.2307/2372560, URL https://www.jstor.org/stable/2372560?origin=crossref.

[19] Kabamba, P. T., and Girard, A. R., *Fundamentals of Aerospace navigation and guidance*, Cambridge University Press, 2014.